General and Comparative Endocrinology 292 (2020) 113441

Contents lists available at ScienceDirect

General and Comparative Endocrinology

journal homepage: www.elsevier.com/locate/ygcen

Stem cell development involves divergent thyroid hormone receptor subtype expression and epigenetic modifications in the *Xenopus* metamorphosing intestine

Takashi Hasebe[a,1], Kenta Fujimoto[a,1], Daniel R. Buchholz[b], Atsuko Ishizuya-Oka[a,*]

[a] Department of Biology, Nippon Medical School, Kyonan-cho, Musashino, Tokyo, Japan
[b] Department of Biological Sciences, University of Cincinnati, Cincinnati, OH, USA

ARTICLE INFO

Keywords:
Stem cell
Thyroid hormone receptor
Intestine
Histone modification
Metamorphosis
Xenopus laevis

ABSTRACT

In the intestine during metamorphosis of the frog *Xenopus laevis*, most of the larval epithelial cells are induced to undergo apoptosis by thyroid hormone (TH), and under continued TH action, the remaining epithelial cells dedifferentiate into stem cells (SCs), which then newly generate an adult epithelium analogous to the mammalian intestinal epithelium. Previously, we have shown that the precursors of the SCs that exist in the larval epithelium as differentiated absorptive cells specifically express receptor tyrosine kinase-like orphan receptor 2 (Ror2). By using Ror2 as a marker, we have immunohistochemically shown here that these SC precursors, but not the larval epithelial cells destined to die by apoptosis, express TH receptor α (TRα). Upon initiation of TH-dependent remodeling, TRα expression remains restricted to the SCs as well as proliferating adult epithelial primordia derived from them. As intestinal folds form, TRα expression becomes localized in the trough of the folds where the SCs reside. In contrast, TRβ expression is transiently up-regulated in the entire intestine concomitantly with the increase of endogenous TH levels and is most highly expressed in the developing adult epithelial primordia. Moreover, we have shown here that global histone H4 acetylation is enhanced in the SC precursors and adult primordia including the SCs, while tri-methylation of histone H3 lysine 27 is lacking in those cells during metamorphosis. Our results strongly suggest distinct roles of TRα and TRβ in the intestinal larval-to-adult remodeling, involving distinctive epigenetic modifications in the SC lineage.

1. Introduction

In the adult mammalian intestine, the epithelium is rapidly renewed from stem cells (SCs) which are localized in the crypt throughout the adulthood (Clevers, 2013; Koo and Clevers, 2014). Accumulating evidence indicates that niche signals including Wnts and Notch play important roles in homeostasis of the adult intestinal epithelium by regulating the SCs (Beumer and Clevers, 2016; Farin et al., 2016). However, it still remains poorly understood how the SCs and their niche are formed in the intestine during postembryonic development.

In the *Xenopus laevis* intestine during metamorphosis, most of the larval epithelial cells (larval cells proper) undergo apoptosis, and the remaining cells (SC precursors) dedifferentiate into the SCs (Ishizuya-Oka et al., 2009, 2010) that express leucine-rich repeat-containing G protein-coupled receptor 5 (LGR5), a typical mammalian intestinal SC marker (Sun et al., 2010). The SCs actively proliferate during stages 60–62 (Nieuwkoop and Faber, 1967; early period of metamorphic climax) and then, as morphogenesis of intestinal folds proceeds, differentiate into the simple columnar epithelium that is continuously renewed along the trough-crest axis of the folds (Hourdry and Dauca, 1977; Shi and Ishizuya-Oka, 1996), similar to the mammalian counterpart that is renewed along the crypt-villus axis throughout adulthood (Cheng and Bjerknes, 1985; Madara and Trier, 1994). Considering that this larval-to-adult intestinal remodeling can be experimentally induced by thyroid hormone (TH) both *in vivo* and *in vitro* (Ishizuya-Oka and Hasebe, 2013; Shi and Ishizuya-Oka, 1996), the *X. laevis* intestine provides us a valuable opportunity to study molecular mechanisms underlying intestinal SC development.

Using this animal model, we previously found that the SC precursors specifically express receptor tyrosine kinase-like orphan receptor 2

Abbreviations: AcH4, acetylation of histone H4; H3K27me3, tri-methylation of histone H3 lysine 27; KO, knock-out; Ror2, receptor tyrosine kinase-like orphan receptor 2; SC, stem cell; ST3, stromelysin-3; Tg, transgenic; TH, thyroid hormone; TR, thyroid hormone receptor; WT, wild-type

* Corresponding author at: Atsuko Ishizuya-Oka, Department of Biology, Nippon Medical School, 1-7-1 Kyonan-cho, Musashino, Tokyo 180-0023, Japan.
E-mail address: a-oka@nms.ac.jp (A. Ishizuya-Oka).

[1] Contributed equally.

https://doi.org/10.1016/j.ygcen.2020.113441
Received 8 November 2019; Received in revised form 22 January 2020; Accepted 16 February 2020
Available online 18 February 2020

(Ror2), although they are differentiated as absorptive epithelial cells possessing the brush border and are not morphologically distinguished from the rest of the larval absorptive epithelial cells (Ishizuya-Oka et al., 2014). At stage 60 when Wnt5a, a major ligand of Ror2, is up-regulated by endogenous TH, the SC precursors change in shape from simple columnar to roundish via Wnt5a/Ror2 signaling, which is essential for their dedifferentiation into the SCs (Ishizuya-Oka et al., 2014). Thus, the *X. laevis* tadpole intestine, where the SC precursors can be easily identified by using Ror2 as a marker, serves as a unique and excellent model for investigating how the SCs and their niche are formed during postembryonic development.

It is well established that the actions of TH are mediated by nuclear thyroid hormone receptor (TR). In *Xenopus* tadpoles, TR activation has been shown to be necessary for normal intestinal remodeling (Buchholz et al., 2004; Choi et al., 2017; Hasebe et al., 2011), which also likely requires corticosterone and/or insulin signaling (Ishizuya-Oka and Shimozawa, 1991; Sachs and Buchholz, 2019). In addition, a growing body of evidence indicates that TR epigenetically regulates the expression of numerous TH response genes at least partly by changing histone modifications in a TH-dependent manner (Bilesimo et al., 2011; Kasai et al., 2015; Matsuura et al., 2012; Shi, 2013; Wen et al., 2017). Nevertheless, in the *X. laevis* intestine, little is known about TR expression or histone modifications in SC precursors and descendent cells during metamorphosis.

There are two subtypes of TR, TRα and TRβ, in amphibians as in mammals. Previous studies have shown different expression profiles of TRα and TRβ mRNAs in different organs during *X. laevis* metamorphosis. Basically, TRα mRNA is pervasively expressed throughout the larval period and metamorphosis and is predominantly expressed in adult-specific organs such as the hind limb (Wen and Shi, 2016; Wong and Shi, 1995). In contrast, TRβ mRNA is transiently up-regulated during metamorphic climax, concomitantly with the rise of endogenous TH levels, and is predominantly expressed in larva-specific organs such as the tail and gills (Furlow et al., 2004; Wang et al., 2008). In the larval-to-adult remodeling intestine, although both TRα and TRβ mRNAs are expressed at the organ level during metamorphosis (Wong and Shi, 1995), it still remains unknown whether expression profiles of TRα and TRβ are different in the SC lineage as compared to the larval cells proper. To address this issue, in the present study, we examined the expression of TRα and TRβ among these epithelial cell types using transgenic (Tg) tadpoles expressing GFP under the control of the Ror2 promoter. We found that TRα is expressed in SC precursors but not larval cells proper, whereas TRβ expression is transiently up-regulated in both the SCs and larval cells proper. In addition, by using acetylation of histone H4 (AcH4) and tri-methylation of histone H3 lysine 27 (H3K27me3) as active and repressive histone marks, respectively (Li et al., 2007; Swigut and Wysocka, 2007), we immunohistochemically examined changes in histone modifications in each cell type during metamorphosis and found that global AcH4 levels increase with higher levels of the TR expression in the proliferating SCs. Our findings imply distinct roles of TRα and TRβ in intestinal remodeling, involving divergent epigenetic regulation in the SC lineage.

2. Materials and methods

2.1. Animals and generation of transgenic tadpoles

Tadpoles of the South African clawed frog (*Xenopus laevis*) at stages from 54 (Nieuwkoop and Faber, 1967; premetamorphosis) to 66 (end of metamorphosis) were reared in the laboratory and were used throughout the experiments. To generate transgenic (Tg) tadpoles expressing EGFP under the promoter of Ror2, we isolated Ror2.L genomic regions which were thought to regulate the expression of this gene. Based on the ChIP-seq data for H3K27ac (http://www.xenbase.org/common/jsp/showGBrowse.jsp?xl9_1/?name=chr1L:137201336-137294075), we chose 2 regions in Ror2.L genome (from the upstream of the Ror2.L gene to 1st intron and around 2nd exon) as the promoter. By using the *X. laevis* genomic DNA extracted from the intestine at stage 62, PCR was performed with primers (5′-TTGACTGTTTTGTGCATAAC TAAATG-3′ and 5′-GATTTTGATCGACTATCTCCCCAAAC-3′) followed by nested PCR with primers containing the restriction enzyme (RE) recognition sites (5′-AATATAGCGGCCGCGCTAGCGTTACAAACTAGAA ACACTTCGGG-3′ and 5′-AATATAACTAGTAGCGTGTTTTCCCATAGGC TACAATG-3′) to obtain a DNA fragment consisting of the upstream region (680 bp), 1st exon (91 bp) and 1st intron (partial, ca. 4.4 kb) of Ror2.L. This fragment was double-digested with NotI and SpeI, inserted into pBSII-KS+ predigested with the same REs and sequenced. Since there were 3 “ATG” triplets in the 1st exon (5′-ATGTCCAGGACCAGG AGCCAGAATGGGGGGATTGGATG-3′), they were mutated by 2-step PCR to avoid undesired translation initiation (mutated sequence: 5′-TTGTCCAGGACCAGGAGCCAGAAAGGGGGGATTGGTTG-3′) (pBSII-KS+_Ror2L-Up-Int1-mut). To obtain the other DNA fragment consisting of downstream region of 1st intron (491 bp) and 2nd exon (partial, 23 bp), PCR was performed with primers (5′-CTGTGTAATATCTAAGG AAAATAAGC-3′ and 5′-ATGCCTCCACTTTTAGAAGAGCATGG-3′) followed by nested PCR with primers containing the RE recognition sites (5′-AATATATCTAGAGCATTTTTGAGTGATAATTCAGC-3′ and 5′-AATAT ACTCGAGTTCGAAGTCCCAGTGGGTCATTCAAG-3′). This fragment was double-digested with XbaI and XhoI, inserted into pBSII-KS+ predigested with the same REs and sequenced. Since 2nd exon contained 1 “ATG” triplet (5′-GTGAAATGGAAATACCAGACTT-3′), this was mutated to “TTG” by PCR (pBSII-KS+_Ror2L-Int1d-Ex2mut). The DNA fragment (531 bp) digested out from pBSII-KS+_Ror2L-Int1d-Ex2mut by XhoI and XbaI was inserted into pBSII-KS+_Ror2L-Up-Int1-mut predigested with XhoI and SpeI to integrate the cloned DNA fragments (pBSII-KS +_Ror2LReg1). This integrated DNA fragment was used as the Ror2 promoter. Finally, the DNA construct containing Ror2 promoter driving EGFP, γ-crystallin promoter driving GFP3 (Fu et al., 2002) and Tol2 transposase recognition sequences at both ends of the whole construct was generated (pDG-Ror2LReg1EG-Tol2(ITR); the sequence information has been deposited in GenBank, accession: MN025426) and used for transgenesis.

Fertilized *X. laevis* eggs were prepared as previously described (Hasebe et al., 2007) and injected with pDG-Ror2LReg1EG-Tol2(ITR) together with either Tol2 mRNA or Tol2 protein (Hamlet et al., 2006; Ni et al., 2016; Shibano et al., 2007). The Tg tadpoles were identified by GFP3 expression in the eye under a fluorescence dissecting microscope and reared to the appropriate developmental stages.

At least three tadpoles were analyzed for each stage. All experiments involving the *X. laevis* animals were approved by the Animal Use and Care Committee of Nippon Medical School.

2.2. Quantitative real-time reverse transcription-polymerase chain reaction (qRT-PCR)

Total RNA was extracted from the small intestine at the indicated developmental stages by using TRI Reagent (Molecular Research Center, Cincinnati, OH, USA) followed by DNase treatment with DNA-free (Ambion, Austin, TX, USA) to remove any DNA contamination. The integrity of RNA was checked based on 18S and 28S ribosomal RNAs by electrophoresis. Total RNA was mixed with GoTaq 1-Step RT-qPCR System (Promega, Madison, WI, USA), and then quantitative real-time RT-PCR was performed by using PikoReal 96 Real-Time PCR System (Thermo Fisher Scientific, Waltham, MA, USA) according to the manufacturer’s instructions. The primer pairs used are: 5′-TCCCCAACACC ACCAAAAGGC-3′ and 5′-TCTGTTCCCCTCCCGATATTGAAG-3′ for TRα.L (GenBank: NM_001088126), 5′-CTGACTGAACTGAGGCAGGG-3′ and 5′-CAATGTTGGACTTGGCACGG-3′ for TRβ.L (GenBank: NM_001096713. The entire mRNA sequence is available at http://gbrowse.xenbase.org/fgb2/gene_model_details/xl9_1?feature_id=681956), 5′-GCCGTGGTGCTCCTCTTGCC-3′ and 5′-TGCCACAGTACAC AAACTGTCCG-3′ for ribosomal protein L8 (rpL8.S; GenBank:

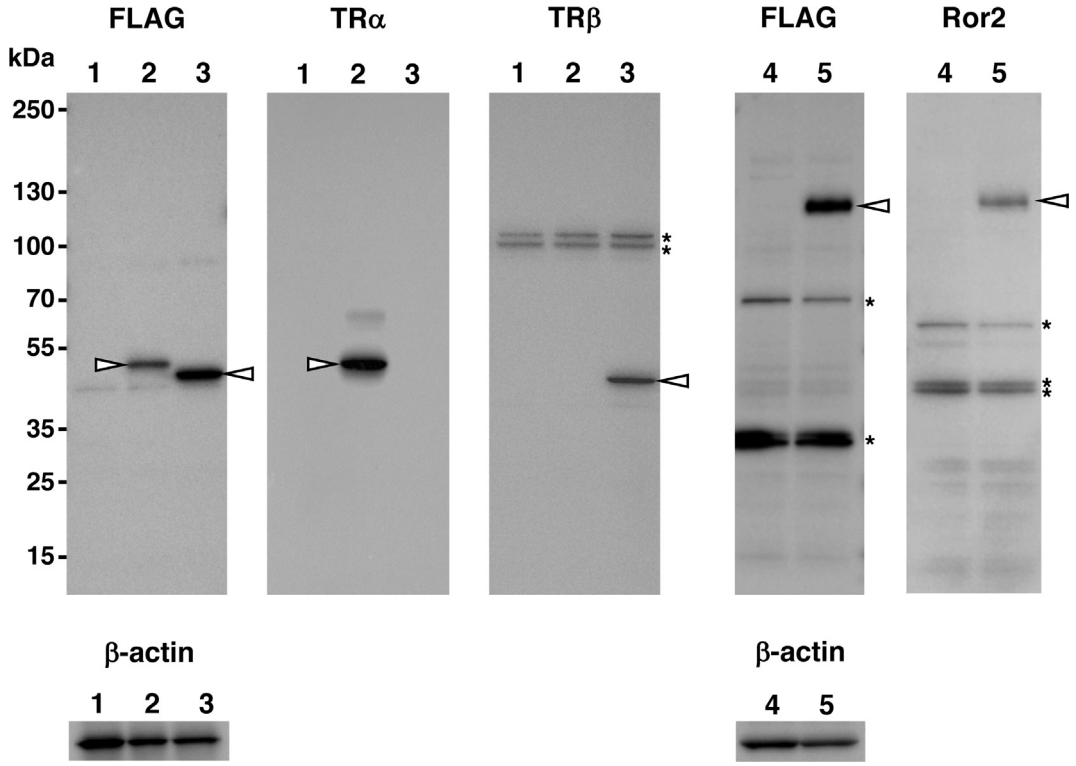

Fig. 1. The rabbit or mouse antibodies against human TRα, TRβ, and Ror2 cross-react with *X. laevis* TRα, TRβ, and Ror2 proteins, respectively. *In vitro*-translated (IVT) proteins (1. Non-template control, 2. FLAG-TRα, 3. FLAG-TRβ) and proteins extracted from *X. laevis* embryos (4. uninjected, 5. Ror2-FLAG mRNA-injected) were analyzed by Western blotting to detect the indicated peptide/protein. Arrowheads indicate the specific signals with the expected molecular weight. Asterisks indicate non-specific signals as they are also detected in the negative control. The mouse anti-human β-actin antibody was used for the loading control.

NM_001086996). The level of specific mRNA was normalized against the level of rpL8.S mRNA (Hasebe et al., 2017a; Shi and Liang, 1994) for each sample. The samples were analyzed in duplicate 3 times. The specificity of the amplification was confirmed by the dissociation curve analysis and gel electrophoresis. The results were analyzed by ANOVA followed by Scheffe's post hoc test.

2.3. Cloning of X. laevis genes and Western blot analysis

TRα.L was cloned by PCR by using a cDNA from the intestine at stage 62 as a template with primers (5′-GGGAGATTGTTTCCTCTCAGT CTG-3′ and 5′-CTATCATTTGCATATGGGGTACAG-3′) followed by nested PCR with primers containing RE recognition sites (5′-AATATC TCGAGGGAGATTGTTTCCTCTCAGTCTGTATCC-3′ and 5′-AAATCCCG GGCTATCATTTGCATATGGGGTACAGAAGAG-3′). The amplified DNA fragment was double-digested with XhoI and XmaI, inserted into pBSII-KS+ predigested with the same REs and sequenced (pBSII-KS +_TRα.L). The coding region (CDR) of TRα.L was amplified by PCR by using pBSII-KS+_TRα.L as a template with primers containing RE recognition sites (5′-AATATTACCGGTGCCGCCACCATGGACTACAAGGA TGACGACGACAAGGACCAGAATCTCAGCGGGCTGGAC-3′ and 5′-TATT ACTAGTCTAAACTTCCTGGTCCTCAAAGACCTCAAG-3′) to fuse a FLAG epitope tag at the N-terminus. The amplified DNA fragment was double-digested with AgeI and SpeI, inserted into pT7Ts vector (Hasebe et al., 2007) predigested with the same REs and sequenced (pT7Ts_FLAG-TRα.L). In a similar way, TRβ.L was isolated with following primers (For 1st PCR: 5′-TGCAAATTGGGATCTATCCTGG-3′ and 5′-TGCTGAGA ATCCAGAAGCACAG-3′, for nested PCR: 5′-AATATCTCGAGTGCAAAT TGGGATCTATCCTGGG-3′ and 5′-AAATCCCGGGTGCTGAGAATCCAGA AGCACAGTC-3′, for CDR cloning and fusion of FLAG tag at the N-terminus: 5′-AATATTACCGGTGCCGCCACCATGGACTACAAGGATGACGA CGACAAGCCAAGCAGTATGTCAGGGTATATAC-3′ and 5′-TATTACTAG TCTAGTCCTCAAACACTTCCAAGAACAGTG-3′). Then, pT7Ts_FLAG-TRβ.L was obtained. Using these constructs as the templates, FLAG-tagged TRα.L and TRβ.L proteins were produced by TNT T7 Quick Coupled Transcription/Translation System (Promega, Madison, WI, USA) according to the manufacturer's instructions. The *in vitro*-translated (IVT) samples were diluted 1:1 by 2x SDS sample buffer and boiled for 5 min. After centrifugation at 15,000×*g* for 5 min, the supernatant (5 μL each) was used for Western blot analysis. It has been shown that epitope-tagging at an appropriate region of the protein does not affect recognition by the antibody against the wild-type (untagged) one (Suh et al., 2013).

Cloning of Ror2 (accession: NM_001088843, L-homeolog) and construction of pT7Ts_Ror2-FLAG has been previously described (Ishizuya-Oka et al., 2014). By using this plasmid as the template, the capped mRNA encoding FLAG-tagged Ror2 was synthesized with mMESSAGE mMACHINE kit (Thermo Fisher Scientific, Waltham, MA, USA) according to the manufacturer's instructions. The synthesized mRNA was injected into one blastomere of 2-cell stage embryos. One day after injection, proteins were extracted from the embryos with IP buffer (20 mM HEPES, pH 7.5, 5 mM KCl, 1.5 mM $MgCl_2$, 1 mM EGTA, 10 mM β-glycerophosphate, 50 mM NaCl, 0.1% IGEPAL) supplemented with protease inhibitor cocktail (Roche Applied Science, Manheim Germany). After centrifugation at 15,000×*g* for 15 min at 4°C, the supernatant was diluted 1:1 by 2x SDS sample buffer and boiled for 5 min. After centrifugation at 15,000×*g* for 5 min, the supernatant (10 μL) was used for Western blot analysis.

The protein samples were electrophoresed on a 5–20% polyacrylamide gel (Anatech, Tokyo, Japan) followed by transferring onto PVDF membrane (Bio-Rad, Hercules, CA, USA). The membrane was immediately washed with Tris-buffered saline (TBS) containing 0.1% Tween-20 (TBST), blocked with 5% skim milk (Fujifilm Wako Pure Chemical, Osaka, Japan) in TBST for 30 min, and incubated overnight at 4°C with the primary antibody (indicated below) diluted in TBST-0.5% milk. After washing 3 times with TBST, the membrane was

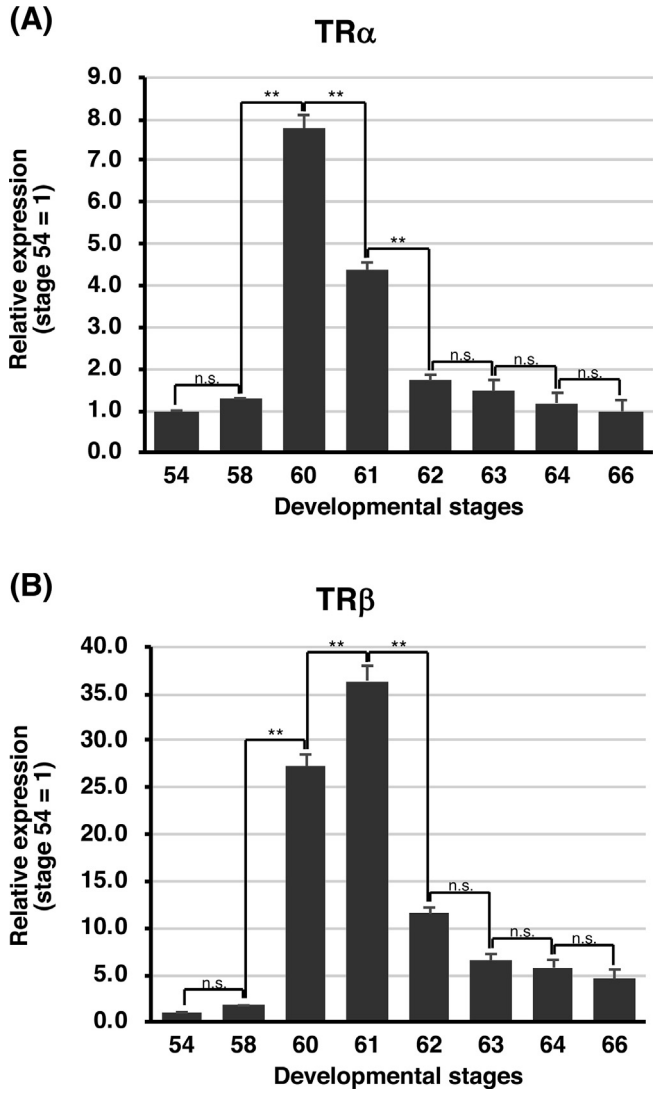

Fig. 2. Expression of TRα and TRβ mRNAs in the small intestine during metamorphosis. Total RNA was prepared from the intestine of *X. laevis* tadpoles at indicated developmental stages and was analyzed by qRT-PCR. Levels of TRα (A) and TRβ mRNAs (B) are shown relative to those of ribosomal protein L8 (rpL8.S) mRNA, with the values at stage 54 set to 1. Error bars represent the SEM (n = 3). The values were analyzed by ANOVA followed by Scheffe's post hoc test, and the results are shown only for the adjacent developmental stages. Asterisks indicate that the mRNA levels are significantly different. **: $P < 0.01$, n.s.: not significant.

incubated for 1 h at room temperature with the secondary antibody against either mouse or rabbit IgG conjugated with peroxidase (diluted 1:5000, GE Healthcare, Buckinghamshire, England). After washing 3 times with TBST, peroxidase activity was detected by using ImmunoStar (Fujifilm Wako Pure Chemical) with an imaging system Ez-Capture MG (Atto, Tokyo, Japan).

Since anti-TR antibodies were generated from human immunogens but not *Xenopus* ones, we confirmed their specificities for *Xenopus* TR proteins produced above. The rabbit anti-TRα antibody (diluted 1:500; GTX25621, GeneTex, Irvine, CA, USA) specifically recognized the *X. laevis* TRα protein, whereas the mouse anti-TRβ antibody (diluted 1:500; GTX22743, GeneTex) recognized the *X. laevis* TRβ protein by Western blot analysis (Fig. 1). We also confirmed that the rabbit anti-Ror2 antibody (diluted 1:400; MBS2028051, MyBioSource, San Diego, CA, USA) specifically recognizes the *X. laevis* Ror2 protein (Fig. 1) and that the immunohistochemical staining of the *X. laevis* intestine with this antibody (see below) showed the same expression pattern as that reported previously (Ishizuya-Oka et al., 2014). The mouse anti-FLAG M2 antibody (diluted 1:1000, Sigma-Aldrich) was used for the control experiments. As a loading control for protein input of each sample, the mouse monoclonal anti-human β-actin antibody (Abcam, Tokyo, Japan) was used (diluted 1:1000). We confirmed that almost equal amount was loaded on each lane. In addition, to perform Western blot analysis in more natural conditions, IVT protein samples were prepared in a non-reducing and non-denaturing sample buffer. They were separated by native PAGE followed by Western blotting to check whether mouse anti-TRβ antibody recognized the non-denatured form of *X. laevis* TRβ protein (Fig. S1A). Furthermore, to confirm the antigen-binding specificity of the anti-TRβ antibody, Western blotting of the intestinal homogenates was performed using the antibody preabsorbed with recombinant *X. laevis* TRβ protein. Briefly, to prepare the recombinant *X. laevis* TRβ protein, a DNA fragment consisting of T7 promoter, ribosome-binding site and FLAG-tagged *X. laevis* TRβ coding sequence was generated by PCR and used as the template for PURExfrex 2.0 *in vitro* translation system (GeneFrontier, Chiba, Japan). The FLAG-TRβ was purified by anti-FLAG M2 affinity gel (Sigma-Aldrich) at 4°C for 2 h. The TRβ-bound affinity gel was then mixed with PBST-0.5% milk containing the anti-TRβ antibody and incubated overnight at 4°C. This mixture was centrifugated to remove the gel and used as the preabsorbed solution for Western blot to detect the endogenous TRβ in the total protein extracted from the *X. laevis* intestine at stage 61. To prepare the non-absorbed control solution, *in vitro* translation by PURExfrex was done without DNA template followed by the same procedures described above. We observed a reduced signal by preabsorption (Fig. S1B). These results convinced us that this antibody could be used for the immunohistochemical analysis.

2.4. Immunohistochemistry

Tubular fragments were isolated from the anterior part of the wild-type (WT) and Tg small intestines just posterior to the bile duct junction, fixed with 95% ethanol at 4°C for 4 h, embedded in paraffin, and cut at 5 μm. Some sections of the WT intestines were immersed in 1% H_2O_2 at room temperature for 15 min to inactivate endogenous peroxidase and incubated with the following antibodies at room temperature for 1 h: the rabbit anti-TRα antibody (diluted 1:100), the mouse anti-TRβ antibody (diluted 1:20), and the rabbit anti-histone H4K5K8K12K16ac (AcH4) (diluted 1:400; GeneTex) and anti-histone H3K27me3 (diluted 1:200; GeneTex) antibodies, whose epitopes are 100% and more than 97% similar to the *X. laevis* counterparts, respectively (manufacturers' information). The sections were then incubated with biotin-labeled anti-IgG and peroxidase-conjugated streptavidin (Nichirei, Tokyo, Japan) followed by 0.02% 3, 3′-diaminobenzidine-4HCl (DAB) and 0.006% H_2O_2.

In addition, to distinguish conveniently between the adult epithelial primordia and the larval epithelial cells proper during stages 60–62, some sections adjacent to those used for immunohistochemical analysis were stained with methyl green-pyronine (MG-P) (Muto, Tokyo, Japan) for 5 min. We have previously shown that the adult epithelial primordia are intensely stained red with pyronine because of their RNA-rich cytoplasm, whereas the staining intensity of the larval cells proper undergoing apoptosis becomes much weaker (Ishizuya-Oka et al., 2000; Ishizuya-Oka and Ueda, 1996). Furthermore, some sections of the Tg intestines were double-immunostained at room temperature for 1 h with the mixtures of the mouse anti-GFP (diluted 1:50; MBL, Nagoya, Japan) and the rabbit antibody against Ror2 (diluted 1:10), TRα (diluted 1:50), histone AcH4 (diluted 1:200), or histone H3K27me3 (diluted 1:100). The sections were then incubated for 1 h with a mixture of Alexa Fluor 488-conjugated anti-mouse IgG (1:500; Molecular Probes, Eugene, OR, USA) and Alexa Fluor 568-conjugated anti-rabbit IgG antibodies (1:500; Molecular Probes), counterstained with 4′, 6-diamidino-2-phenylindole, dihydrochloride (DAPI) (10 μg/ml; Dojindo, Kumamoto, Japan), and analyzed by fluorescence microscopy. More than

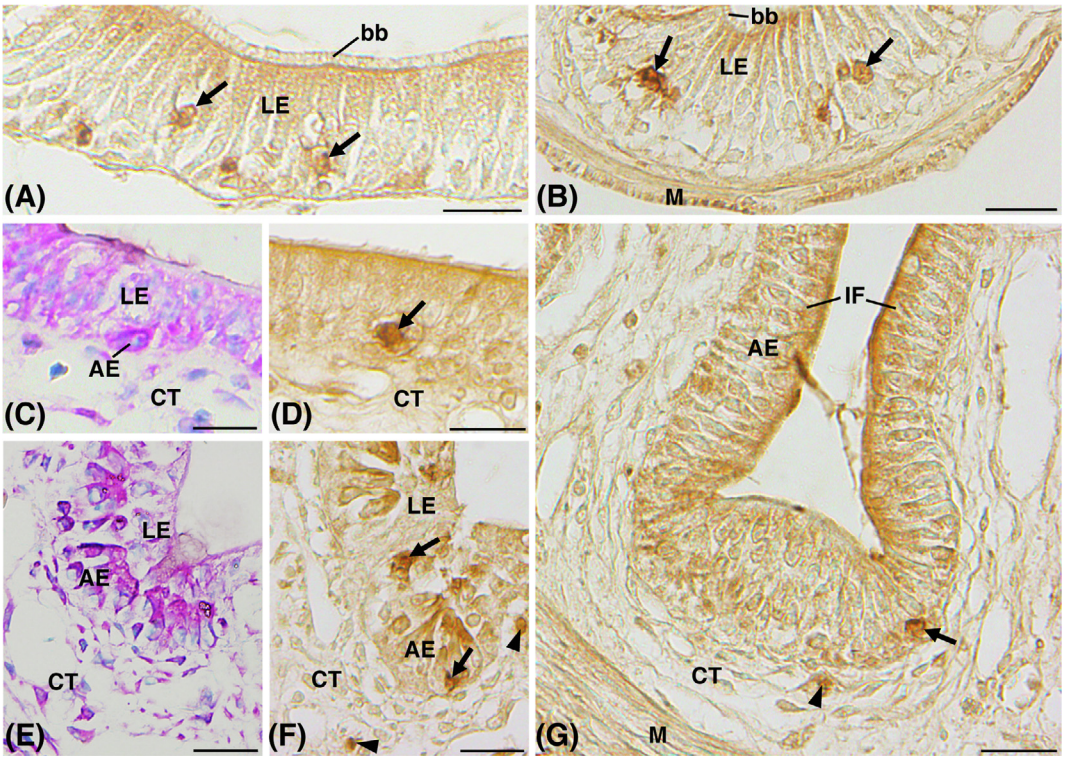

Fig. 3. Expression pattern of TRα in the small intestine during metamorphosis. Cross sections were immunostained with anti-TRα antibody (A, B, D, F, G) or stained with methyl green-pyronine (MG-P) (C, E). (A) Stage 54. (B) Stage 57. The larval epithelium (LE) is simple columnar. Some nuclei of absorptive epithelial cells possessing the brush border (bb) are positive for TRα (arrows in a and b). (C, D) Stage 60. Primordia of the adult epithelium (AE) stained strongly red with MG-P appear between the larval epithelium and the connective tissue (CT) (C), and their nuclei are positive for TRα (arrow in D). (E, F) Stage 61. Nuclei positive for TRα are detectable in the adult epithelial primordia (arrows in F) but not in the degenerating larval epithelium. Nuclei positive for TRα are detectable in the connective tissue (arrowheads in F). (G) Stage 66. Epithelial nuclei positive for TRα are mostly localized in the trough of newly-formed intestinal folds (IF) (arrow). Nuclei positive for TRα are also detectable in the connective tissue (arrowhead). M, muscle. Scale bars = 20 μm.

three tadpoles were examined for each developmental stage. All control sections showed only background levels of signals except for non-specific irregular signals for GFP in the outer surface of the epithelium and TRα in lysosomes of the degenerating larval cells proper during 60–62.

3. Results

3.1. Temporal expression of TRα and TRβ mRNAs during metamorphosis

We first examined the temporal expression of TRα and TRβ mRNAs in the *X. laevis* small intestine during metamorphosis by qRT-PCR. The expression of TRα mRNA was up-regulated and reached its peak at stage 60 (early period of metamorphic climax) and then gradually decreased toward stage 66 (end of metamorphosis) (Fig. 2A). On the other hand, the expression of TRβ mRNA was more drastically up-regulated at stage 60 and then reached its peak at stage 61, a stage later than TRα. Thereafter, the expression gradually decreased toward stage 66 (Fig. 2B).

3.2. Different expression patterns of TRα and TRβ proteins during intestinal remodeling

We next immunohistochemically examined the expression of TRα and TRβ in the *X. laevis* small intestine at the cellular level during metamorphosis. During stages 54–59, the larval epithelium remains simple columnar and is surrounded by the immature connective tissue, which is very thin except for a single fold, the typhlosole. A small number of cells immunoreactive for TRα were randomly distributed in the entire larval epithelium. They were morphologically identified as absorptive epithelial cells possessing the brush border, and the immunoreactivity for TRα was localized in their nuclei (Fig. 3A and B). At stage 60, SCs appear as small islets strongly stained red with MG-P between the larval epithelium and the developing connective tissue (Fig. 3C) (Ishizuya-Oka et al., 2003). The immunoreactivity for TRα was detectable in nuclei of such primordia of the adult epithelium (Fig. 3D). Then, during stages 61–62, the adult epithelial primordia rapidly grow in size by active proliferation (Fig. 3E) (Ishizuya-Oka and Ueda, 1996). The nuclei immunoreactive for TRα remained localized in the adult epithelial primordia, although their number was limited (Fig. 3F). In contrast, no nuclei immunoreactive for TRα were detected in the remaining larval epithelium (larval cells proper). Thereafter, as morphogenesis of multiple intestinal folds proceeds, the adult epithelial primordia replace the larval cells proper and differentiate into the simple columnar epithelium. At stage 66, the epithelial nuclei immunoreactive for TRα became mostly localized in the trough of the intestinal folds (Fig. 3G), where the SCs reside (Ishizuya-Oka et al., 2003; Sun et al., 2010). In the connective tissue, nuclei immunoreactive for TRα were randomly detected, but their number was small throughout metamorphosis (Fig. 3F and G).

On the other hand, the immunoreactivity for TRβ was very weak until stage 55 (Fig. 4A), and then slightly increased in intensity in nuclei of the larval epithelium (Fig. 4B). At stage 60 when the adult epithelial primordia appear, the immunoreactivity for TRβ suddenly increased in intensity in the entire epithelium and the connective tissue, in agreement with the rapid increase of TRβ mRNA by qRT-PCR. The immunoreactivity was detected in a variety of cells at various intensities but most strongly in the adult epithelial primordia where the cytoplasm was often positive for TRβ (Fig. 4C), suggesting active TRβ synthesis during this period. Then, during stages 61–62, the nuclei immunoreactive for TRβ gradually increased in number in the adult

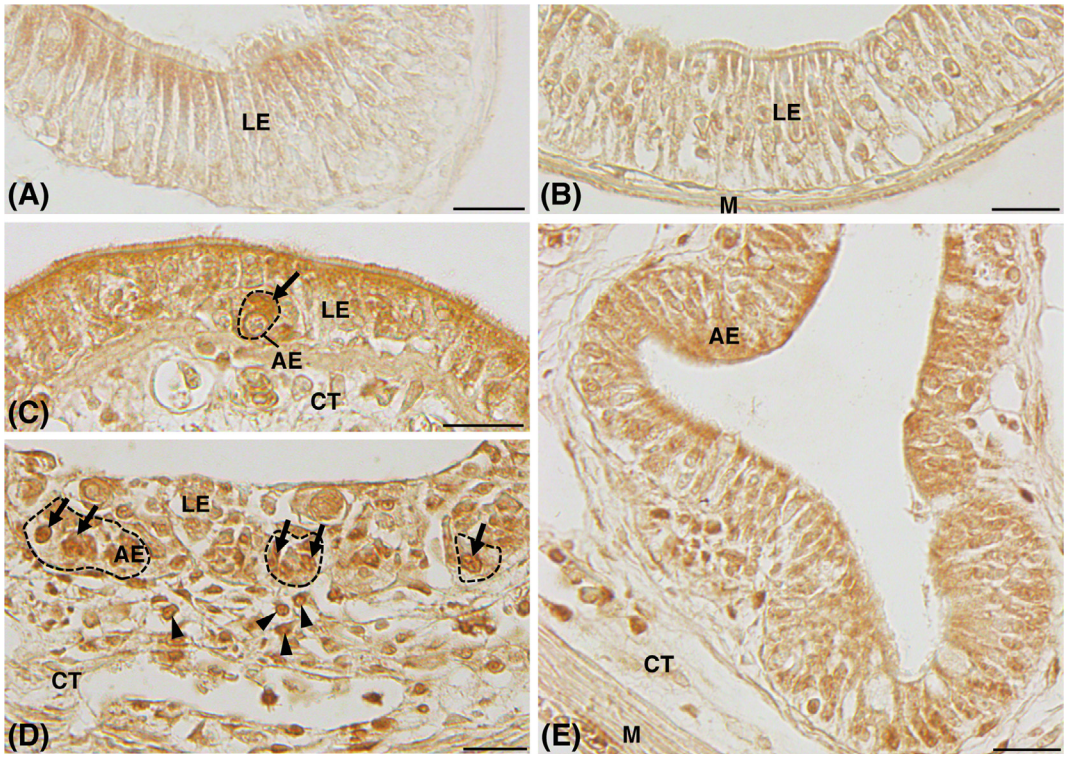

Fig. 4. Expression pattern of TRβ in the small intestine during metamorphosis. Cross sections were immunostained with anti-TRβ antibody. (A) Stage 54. The immunoreactivity for TRβ is very weak, if any, in the larval epithelium (LE). (B) Stage 57. Some nuclei of the larval epithelium are very weakly positive for TRβ. (C) Stage 60. The cytoplasm of the adult epithelial primordia (AE; dashed line) is highly positive for TRβ (arrow). (D) Stage 61. Most of the nuclei in the adult epithelial primordia (dashed lines) are positive for TRβ (arrows). In addition, some nuclei of the connective tissue (CT) are positive for TRβ (arrowheads). (E) Stage 66. Nuclei positive for TRβ are occasionally detectable in the entire adult epithelium and the connective tissue. M, muscle. Scale bars = 20 μm.

epithelial primordia and the developing connective tissue, but decreased in the larval cells proper (Fig. 4D). Thereafter, as the intestinal folds form, the immunoreactivity for TRβ gradually decreased in intensity and at stage 66, a small number of nuclei immunoreactive for TRβ were randomly detected in the entire epithelium and the connective tissue (Fig. 4E).

To examine whether the SC precursors, which specifically express Ror2 (Ishizuya-Oka et al., 2014), coincide with the cells expressing TRα mentioned above or not, we used Tg tadpoles expressing GFP under the control of the Ror2 promoter. We first confirmed by double-immunofluorescence labeling that the cells expressing GFP coexpressed Ror2 in the Tg intestines (Fig. 5A and B). At stage 57, nuclei of the cells expressing GFP, that is, SC precursors, were highly immunoreactive for TRα (Fig. 5C). Then, at stage 61 when the adult epithelial primordia express Ror2, some nuclei of the cells expressing GFP, that is, adult epithelial primordia, were immunoreactive for TRα (Fig. 5D). Thus, TRα is specifically expressed in the SC precursors, and after their dedifferentiation, in the SCs and/or SC progeny.

3.3. Changes in global AcH4 and H3K27me3 levels during intestinal remodeling

We next immunohistochemically examined histone modifications in the *X. laevis* intestine during metamorphosis, by detecting active (AcH4) and the repressive (H3K27me3) histone marks. During stages 54–59, both nuclei immunoreactive for AcH4 (Fig. 6A and C) and those for H3K27me3 (Fig. 6B and D) were randomly detected with various degree of intensity in the entire intestine, although the number for H3K27me3 was much smaller than that for AcH4. Then, during stages 60–62, global AcH4 levels increased in the developing adult epithelial primordia and the connective tissue, but were less in the larval cells proper (Fig. 6E). During this period, almost all of the nuclei in the adult epithelial primordia were strongly immunoreactive for AcH4. In contrast, nuclei immunoreactive for H3K27me3 were never detected in the adult epithelial primordia (Fig. 6F), suggesting that genes in the active chromatin state are predominant in these cells. Characteristically, in the connective tissue, nuclei immunoreactive for H3K27me3 increased in number only in the region surrounding the adult epithelial primordia (Fig. 6F). Thereafter, as the intestinal folds form, the immunoreactivity for AcH4 had less intensity in the entire intestine except for the trough of the intestinal folds (Fig. 6G). On the other hand, a small number of nuclei immunoreactive for H3K27me3 were mostly localized in the tip and trough of the folds (Fig. 6H).

To investigate changes in histone modifications in the SC lineages more precisely, we again used the Tg intestine where the SC precursors/SCs could be easily identified by their GFP expression and performed double-immunofluorescence labeling. At stage 57, nuclei of the cells expressing GFP, that is, SC precursors expressing TRα, were immunoreactive for AcH4 (Fig. 7A) but not for H3K27me3 (Fig. 7C). Then, at stage 61, nuclei of the cells expressing GFP, that is, adult epithelial primordia highly expressing TRβ and TRα, were highly immunoreactive for AcH4 (Fig. 7B) but not for H3K27me3 (Fig. 7D).

4. Discussion

In the present study, we used Tg *X. laevis* intestines to distinguish SC precursors from larval cells proper and examined the expression patterns of TRα and TRβ and changes in histone marks among different intestinal epithelial cell populations during metamorphosis. Our immunohistochemical analyses have shown for the first time, to our knowledge, that dedifferentiation of the SC precursors into SCs is associated specifically with TRα expression and distinctive epigenetic marks, whereas subsequent SC development involves both TRα and TRβ (Figure 8).

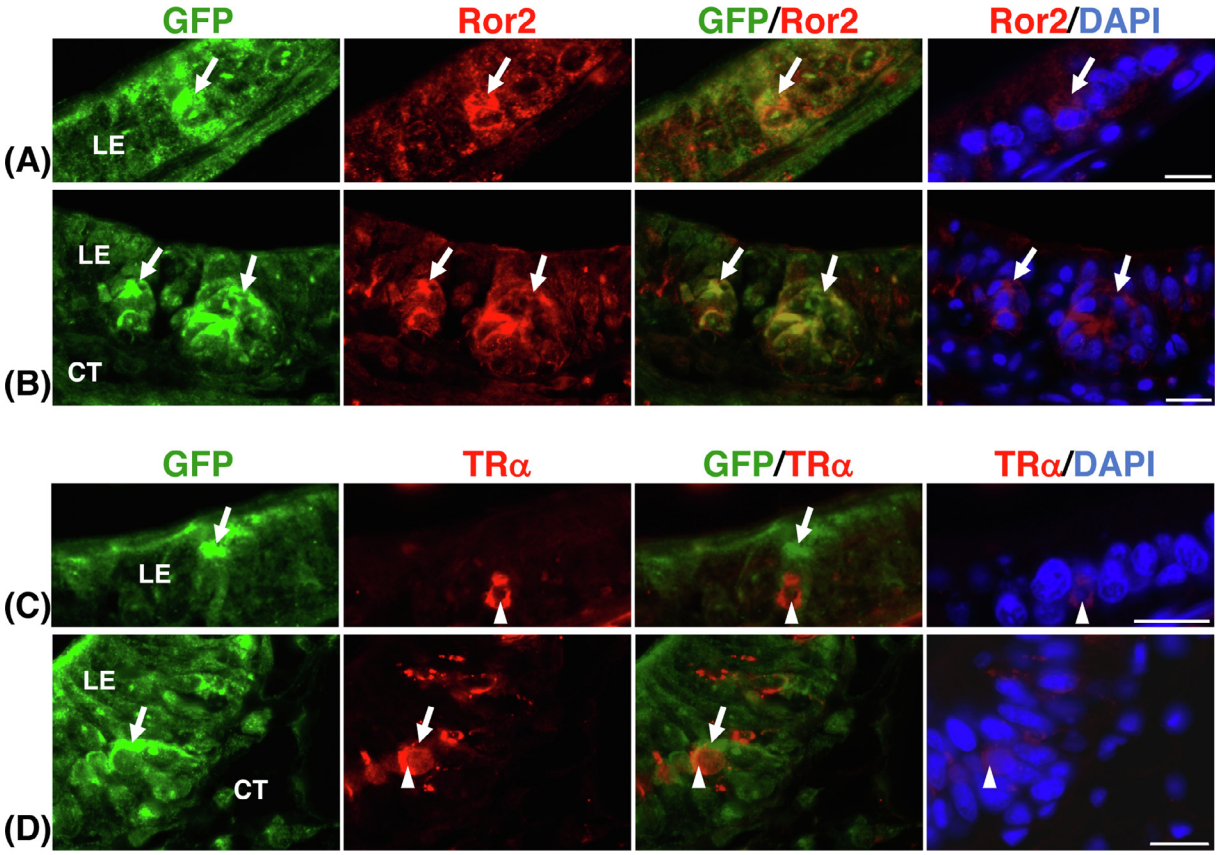

Fig. 5. TRα expression correlates with intestinal SC precursors and proliferating SCs expressing Ror2. Cross sections of the Tg intestine expressing GFP under the control of Ror2 promoter were double-immunostained with anti-GFP (A-D; green) and anti-Ror2 (A, B; red) or anti-TRα (C, D; red) antibodies followed by counterstaining with DAPI (A-D; blue). (A, C) Stage 57. Cells positive for GFP (arrows in A, C) in the larval epithelium (LE) are consistent with SC precursors expressing Ror2 (arrows in A), and their nuclei are positive for TRα (arrowheads in C). (B, D) Stage 61. Cells positive for GFP (arrows in B, D) are consistent with adult epithelial primordial cells positive for Ror2 (arrows in B), and some of their nuclei are positive for TRα (arrowheads in D). CT, connective tissue. Scale bars = 20 μm.

4.1. TRα expression is localized to the adult stem cell lineage in the X. laevis intestine

We have shown here that TRα is highly expressed in SC precursors but not in the larval cells proper. Since the expression of Ror2 has been shown to be up-regulated by TH (Ishizuya-Oka et al., 2014), it seems likely that Ror2 is specifically expressed in the SC precursors via TRα. Then, after their dedifferentiation, TRα remains expressed in the adult epithelial primordia originating from the SC precursors. Thereafter, as the intestinal folds form, TRα expression becomes localized in the trough of the folds where the SCs reside (Ishizuya-Oka et al., 2003; Sun et al., 2010), similar to localization of TRα expression in the crypt of the adult mammalian intestine (Sirakov et al., 2013). On the other hand, TRβ expression is transiently and dramatically up-regulated in the entire intestine, concomitantly with the increase of endogenous TH levels during stages 60–62 (Leloup and Buscaglia, 1977; Ranjan et al., 1994), in agreement with the fact that TRβ is a TH direct response gene possessing TH response elements (Shi, 1999). In addition, our observation that TRβ is expressed in a variety of cells and most highly expressed in the developing adult epithelial primordia, whose cytoplasm as well as nuclei becomes immunoreactive for TRβ probably due to active translation, coincides well with the high transient expression of TRβ mRNA during this period shown by a previous *in situ* hybridization study (Shi and Ishizuya-Oka, 1997). These expression patterns of TRα and TRβ proteins not only coincide with those of their mRNAs by qRT-PCR (present study) and Northern blot (Wong and Shi, 1995), but also strongly suggest that TRα regulates dedifferentiation of the SC precursors into the SCs and subsequent SC development and/or maintenance. Lack of TRα delays this process, as seen in TRα knock-out (KO) tadpoles (Choi et al., 2017). On the other hand, TRβ may participate in the development of the SCs after their appearance and may be predominantly responsible for apoptosis of the larval cells proper.

In addition, we also found distinct expression profiles between TRα and TRβ in the connective tissue, where the cells expressing TRβ suddenly increase in number during stages 60–62, while those expressing TRα are limited in number but detectable throughout metamorphosis. Notably, a recent study showed that the expression of stromelysin-3 (ST3), a metalloproteinase that is directly up-regulated by TH in the connective tissue (Ishizuya-Oka et al., 2000; Patterton et al., 1995), was dramatically reduced in the TRα KO *X. tropicalis* intestine (Choi et al., 2017). Taken together, it seems likely that the connective tissue cells expressing TRα (in the present study) can express ST3 via TH/TRα signaling. Since ST3 has been shown to induce larval epithelial apoptosis by activating the extracellular pathway (Fu et al., 2005; Ishizuya-Oka et al., 2010), ST3 secreted from such cells should cause the larval epithelial apoptosis even in the absence of TRβ. This may explain why the larval-to-adult epithelial remodeling occurred in the TRβ KO *X. tropicalis* intestine (Nakajima et al., 2018; Sakane et al., 2018), even though the larval apoptosis is normally induced by TRβ.

4.2. Both TRα and TRβ are involved in gene expression in the adult stem cell lineage through histone modifications

In the present study, we have also shown that changes in global histone modification levels in the adult epithelial lineage correlate with its TR expression and endogenous TH levels during metamorphosis. At stage 57 when low levels of TH are available (Leloup and Buscaglia, 1977), the active AcH4 but not repressive H3K27me3 marks are

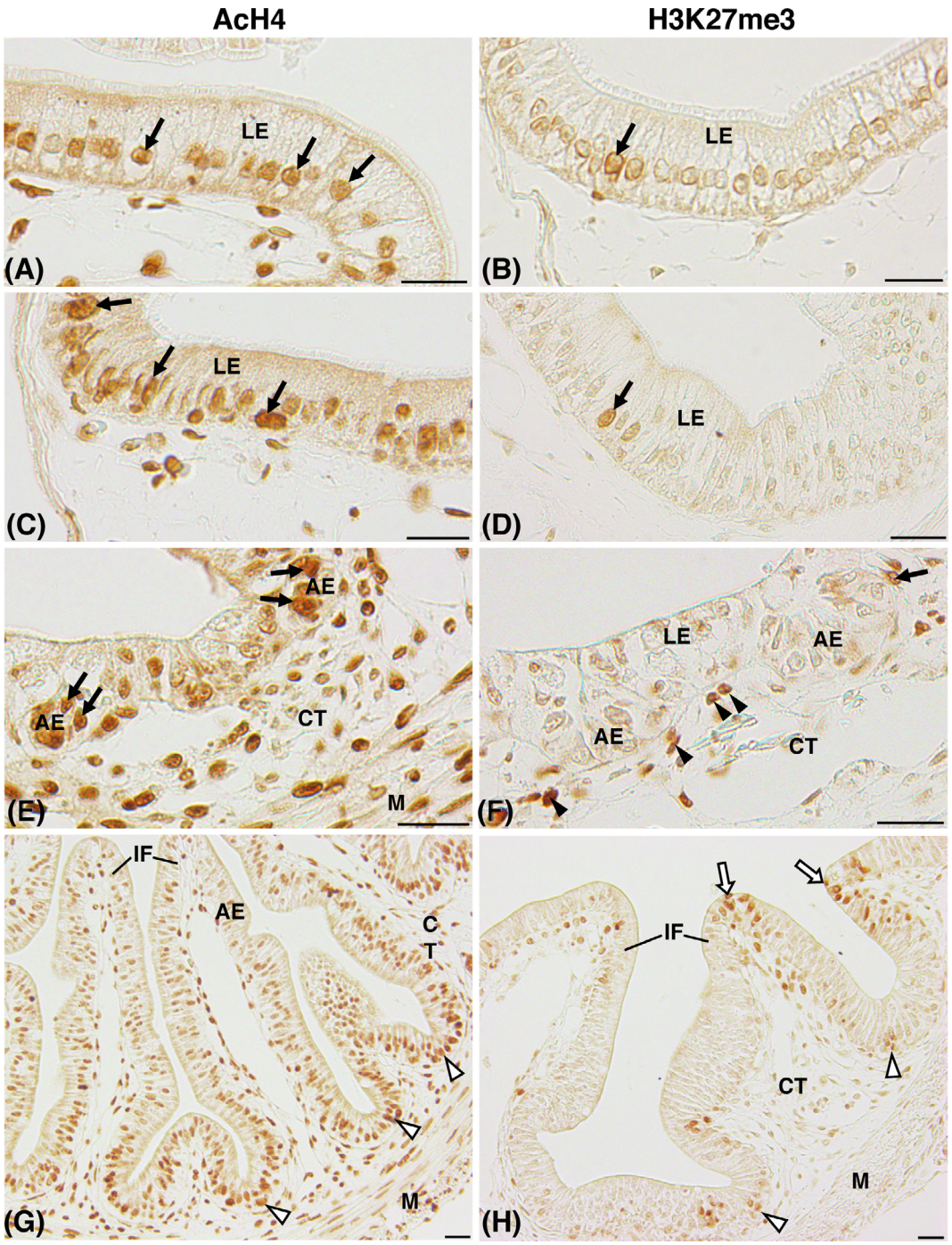

Fig. 6. Changes in global active AcH4 and repressive H3K27me3 levels in the small intestine during metamorphosis. Cross sections were immunostained with anti-AcH4 (A, C, E, G) and anti-H3K27me3 antibodies (B, D, F, H). (A, B) Stage 54. (C, D) Stage 57. Nuclei positive for AcH4 (arrows in A and C) and those for H3K27me3 (arrows in B and D) are randomly distributed in the larval epithelium (LE) with various degree of intensity, although nuclei positive for AcH4 are more numerous than those for H3K27me3. (E, F) Stage 61. Almost all of the nuclei in primordia of the adult epithelium (AE) are highly positive for AcH4 (arrows in E) but negative for H3K27me3 (F). In the connective tissue (CT), numerous nuclei are positive for AcH4 (E), whereas those positive for H3K27me3 are much fewer and mostly localized in the region surrounding the adult epithelial primordia (arrowheads in F). (G, H) Stage 66. Epithelial nuclei highly positive for AcH4 tend to be localized in the trough of the intestinal folds (IF) (arrowheads in G), whereas those for H3K27me3 are mostly localized in their tip (arrows in H) and trough (arrowheads in H). M, muscle. Scale bars = 20 μm.

detectable in the SC precursors expressing TRα. This suggests that TRα activates gene expression in the SC precursors prior to their dedifferentiation and explains well why the appearance of the SCs was delayed in the TRα KO intestine compared to the WT intestine (Choi et al., 2017). Then, during stages 60–62 when the TH levels reach a peak, global AcH4 levels increase in the adult epithelial primordia highly expressing TRβ and TRα. Consistent with this, previous studies reported that the mRNA expression of direct TH response genes such as TH/bZip, Shh, and c-Myc is up-regulated in the adult epithelial primordia during this period (Fujimoto et al., 2012; Hasebe et al., 2008; Ikuzawa et al., 2006; Okada et al., 2017). Thereafter, as the TH levels decrease, AcH4 levels gradually decrease, and its marks become localized in the trough of intestinal folds where the SCs expressing TRα are localized. These correlations between changes in histone modifications and TH/TR

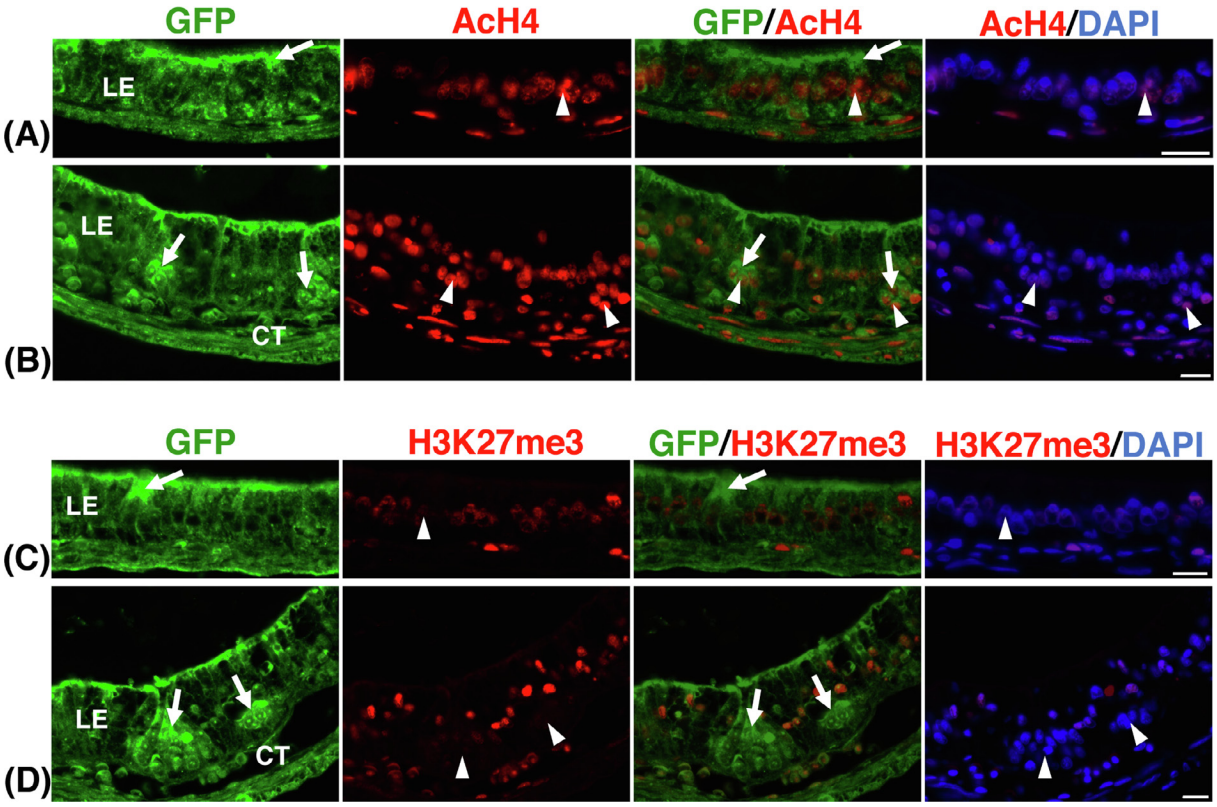

Fig. 7. Active histone modifications in intestinal SC lineages expressing TRs. Cross sections of the Tg intestine were double-immunostained with anti-GFP (A-D: green) and anti-AcH4 (A, B; red) or anti-H3K27me3 antibodies (C, D; red) followed by counterstaining with DAPI (A-D; blue). (A, C) Stage 57. Cells expressing GFP (arrows in A, C) in the larval epithelium (LE), that is, SC precursors expressing TRα, are positive for AcH4 (arrowheads in A) but negative for H3K27me3 (arrowheads in C). (b, d) Stage 61. Adult epithelial primordia expressing GFP (arrows in B, D) are highly positive for AcH4 (arrowheads in B) but negative for H3K27me3 (arrowheads in D). CT, connective tissue. Scale bars = 20 μm.

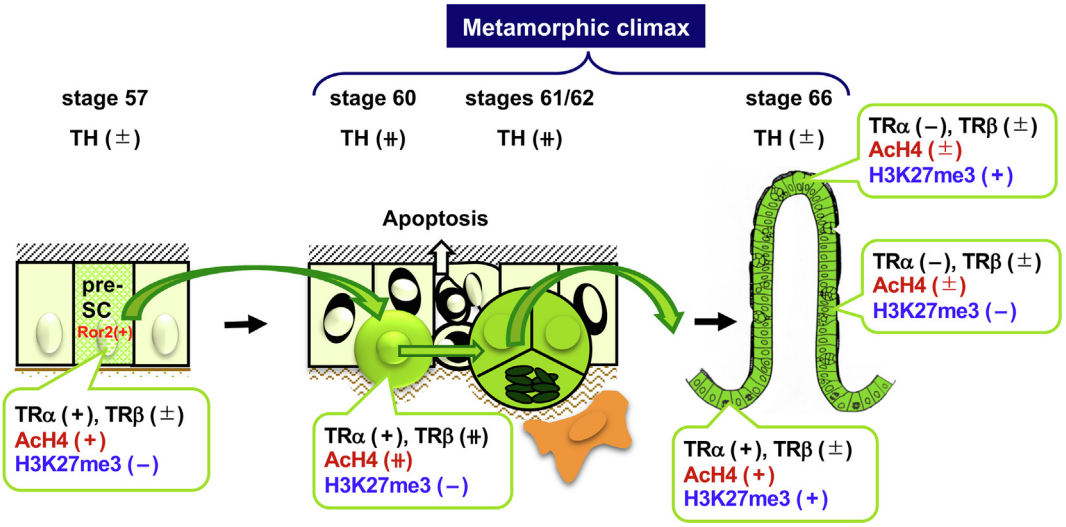

Fig. 8. Schematic illustration showing correlations of TRα and TRβ expression with histone modifications in the SC lineage during the *X. laevis* intestinal remodeling. SC precursors (pre-SCs) that express Ror2 specifically express TRα. In the presence of low TH levels at stage 57, the SC precursors with liganded TRα show active (AcH4) histone marks. After their dedifferentiation into SCs at stage 60, the global AcH4 levels increase in adult epithelial primordia, which consists of the SCs and SC progeny and most highly express TRβ under the highest TH levels. In contrast, repressive H3K27me3 levels remain very low, if any, in the SC precursors and the adult epithelial primordia. At stage 66, both TRα expression and AcH4 marks are localized in the trough of intestinal folds where the SCs reside. On the other hand, H3K27me3 marks are localized in not only the trough but also the tip where epithelial cells undergo apoptosis. The levels are scored as ± , low; + , moderate; ǂ, high.

signaling in the SC lineages agree well with recent evidence that liganded TRs increase active histone marks and decrease repressive ones on TH response genes and their down-stream targets by releasing corepressors and recruiting coactivators including histone acetyltransferases (Grimaldi et al., 2013; Kasai et al., 2015; Matsuura et al., 2012; Paul et al., 2007; Sachs and Buchholz, 2017; Shi, 2013). In addition, we have previously shown by using chromatin immunoprecipitation (ChIP) that those changes mentioned above occur on direct TH response genes such as TH/bZip and TRβ in the metamorphosing *Xenopus* intestine (Buchholz et al., 2005; Matsuura et al.,

2012). In mammalian SCs, a growing body of evidence supports the important roles of histone acetylation in attaining and maintaining stemness (Hirsch et al., 2017). For example, acetylation of histone H4 as well as H3 lysine residues is elevated as somatic cells dedifferentiate into pluripotent SCs (Benevento et al., 2015), whereas global histone H4 acetylation decreases during differentiation of embryonic SCs (Gonzales-Cope et al., 2016). In addition, histone acetyltransferases have been shown to regulate proliferation and differentiation of somatic SCs such as dental pulp (Wang et al., 2014) and hematopoietic SCs (Rebel et al., 2002). Thus, in the *Xenopus* intestine, it is highly possible that TH response genes activated by H4ac in the SC precursors and those in the adult epithelial primordia may be essential for dedifferentiation into the SCs and subsequent SC development, respectively. Identification of such SC-related genes awaits further investigation.

Moreover, in the present study, we found the characteristic profile of the repressive H3K27me3 marks, which are localized in (1) connective tissue cells surrounding the adult epithelial primordia during stages 61–62 and (2) adult epithelial cells in the tip and the trough of intestinal folds at stage 66. In the former case, we have previously shown that such cells near the adult epithelial primordia express multiple signaling molecules including BMP4 essential for SC development (Hasebe et al., 2011, 2017b; Ishizuya-Oka and Hasebe, 2013). Thus, it is highly possible that H3K27me3 represses some genes in the cells to make them differentiate into SC niche cells. On the other hand, in the latter case, the adult epithelial cells at stage 66 have been shown to originate from the SCs localized in the trough of the folds, differentiate, and finally undergo apoptosis in their tip (Hourdry and Dauca, 1977; Ishizuya-Oka and Hasebe, 2013; Shi and Ishizuya-Oka, 1996). Thus, it is tempting to speculate that H3K27me3 in the tip of the folds represses some differentiation genes in the cells for execution of their apoptosis, whereas H3K27me3 in the trough represses some developmental genes in the SCs for their specification as proposed in the mammalian intestine (Kazakevych et al., 2017). Anyway, it should be interesting to investigate what genes are repressed by H3K27me3 in these cells during formation of the SCs and their niche.

4.3. Conclusion

In conclusion, we have shown here that, using the *X. laevis* intestine as a model, different epithelial cell populations differentially express TRα and TRβ, which likely epigenetically regulate gene expression in the SC precursors and proliferating SCs in a TH-dependent manner. Similarly, in the mammalian intestine, a growing body of evidence shows important roles of TH/TR signaling in SC regulation during postembryonic maturation, homeostasis, and tumorigenesis (Frau et al., 2017; Sirakov et al., 2015; Sirakov and Plateroti, 2011), suggesting conserved TH-dependent mechanisms between amphibian and mammalian intestines (Buchholz, 2015). To understand the evolutionarily conserved mechanisms of SC development and regulation, a future challenge will be to sort different epithelial cell populations at different metamorphic stages by using the *X. laevis* Tg intestine and investigate what genes are epigenetically regulated by TRα or TRβ in the SC precursors and subsequent SCs, by using ChIP-seq technology.

CRediT authorship contribution statement

Takashi Hasebe: Conceptualization, Methodology, Investigation, Writing - original draft, Visualization, Funding acquisition. **Kenta Fujimoto:** Conceptualization, Methodology, Investigation, Writing - original draft, Visualization. **Daniel R. Buchholz:** Methodology, Resources, Writing - review & editing. **Atsuko Ishizuya-Oka:** Conceptualization, Methodology, Investigation, Writing - original draft, Visualization, Supervision, Project administration, Funding acquisition.

Declaration of Competing Interest

The authors declare that they have no known competing financial interests or personal relationships that could have appeared to influence the work reported in this paper.

Acknowledgements

We thank M. Kajita for her technical help. We also thank Dr. H. Ogino (Hiroshima Univ.) for his valuable advice about Ror2 promoter.

Funding

This work was supported in part by JSPS KAKENHI Grant Numbers JP17K07475 (to T. H.) and JP18K06320 (to A. I.-O.).

Appendix A. Supplementary data

Supplementary data to this article can be found online at https://doi.org/10.1016/j.ygcen.2020.113441.

References

Benevento, M., Tonge, P.D., Puri, M.C., Nagy, A., Heck, A.J., Munoz, J., 2015. Fluctuations in histone H4 isoforms during cellular reprogramming monitored by middle-down proteomics. Proteomics 15 (18), 3219–3231. https://doi.org/10.1002/pmic.201500031.

Beumer, J., Clevers, H., 2016. Regulation and plasticity of intestinal stem cells during homeostasis and regeneration. Development 143 (20), 3639–3649. https://doi.org/10.1242/dev.133132.

Bilesimo, P., Jolivet, P., Alfama, G., Buisine, N., Le Mevel, S., Havis, E., Demeneix, B.A., Sachs, L.M., 2011. Specific histone lysine 4 methylation patterns define TR-binding capacity and differentiate direct T3 responses. Mol. Endocrinol. 25 (2), 225–237. https://doi.org/10.1210/me.2010-0269.

Buchholz, D.R., 2015. More similar than you think: frog metamorphosis as a model of human perinatal endocrinology. Dev. Biol. 408 (2), 188–195. https://doi.org/10.1016/j.ydbio.2015.02.018.

Buchholz, D.R., Paul, B.D., Shi, Y.-B., 2005. Gene-specific changes in promoter occupancy by thyroid hormone receptor during frog metamorphosis. Implications for developmental gene regulation. J. Biol. Chem. 280 (50), 41222–41228. https://doi.org/10.1074/jbc.M509593200.

Buchholz, D.R., Tomita, A., Fu, L., Paul, B.D., Shi, Y.-B., 2004. Transgenic analysis reveals that thyroid hormone receptor is sufficient to mediate the thyroid hormone signal in frog metamorphosis. Mol. Cell. Biol. 24 (20), 9026–9037. https://doi.org/10.1128/MCB.24.20.9026-9037.2004.

Cheng, H., Bjerknes, M., 1985. Whole population cell kinetics and postnatal development of the mouse intestinal epithelium. Anat. Rec. 211 (4), 420–426. https://doi.org/10.1002/ar.1092110408.

Choi, J., Ishizuya-Oka, A., Buchholz, D.R., 2017. Growth, development, and intestinal remodeling occurs in the absence of thyroid hormone receptor alpha in tadpoles of *Xenopus tropicalis*. Endocrinology 158 (6), 1623–1633. https://doi.org/10.1210/en.2016-1955.

Clevers, H., 2013. The intestinal crypt, a prototype stem cell compartment. Cell 154 (2), 274–284. https://doi.org/10.1016/j.cell.2013.07.004.

Farin, H.F., Jordens, I., Mosa, M.H., Basak, O., Korving, J., Tauriello, D.V., de Punder, K., Angers, S., Peters, P.J., Maurice, M.M., Clevers, H., 2016. Visualization of a short-range Wnt gradient in the intestinal stem-cell niche. Nature 530 (7590), 340–343. https://doi.org/10.1038/nature16937.

Frau, C., Godart, M., Plateroti, M., 2017. Thyroid hormone regulation of intestinal epithelial stem cell biology. Mol. Cell. Endocrinol. 459, 90–97. https://doi.org/10.1016/j.mce.2017.03.002.

Fu, L., Buchholz, D., Shi, Y.-B., 2002. Novel double promoter approach for identification of transgenic animals: a tool for in vivo analysis of gene function and development of gene-based therapies. Mol. Reprod. Dev. 62 (4), 470–476. https://doi.org/10.1002/mrd.10137.

Fu, L., Ishizuya-Oka, A., Buchholz, D.R., Amano, T., Matsuda, H., Shi, Y.-B., 2005. A causative role of stromelysin-3 in extracellular matrix remodeling and epithelial apoptosis during intestinal metamorphosis in *Xenopus laevis*. J. Biol. Chem. 280 (30), 27856–27865. https://doi.org/10.1074/jbc.M413275200.

Fujimoto, K., Matsuura, K., Hu-Wang, E., Lu, R., Shi, Y.B., 2012. Thyroid hormone activates protein arginine methyltransferase 1 expression by directly inducing c-Myc transcription during *Xenopus* intestinal stem cell development. J. Biol. Chem. 287 (13), 10039–10050. https://doi.org/10.1074/jbc.M111.335661.

Furlow, J.D., Yang, H.Y., Hsu, M., Lim, W., Ermio, D.J., Chiellini, G., Scanlan, T.S., 2004. Induction of larval tissue resorption in *Xenopus laevis* tadpoles by the thyroid hormone receptor agonist GC-1. J. Biol. Chem. 279 (25), 26555–26562. https://doi.org/10.1074/jbc.M402847200.

Gonzales-Cope, M., Sidoli, S., Bhanu, N.V., Won, K.J., Garcia, B.A., 2016. Histone H4 acetylation and the epigenetic reader Brd4 are critical regulators of pluripotency in embryonic stem cells. BMC Genomics 17, 95. https://doi.org/10.1186/s12864-016-2414-y.

Grimaldi, A., Buisine, N., Miller, T., Shi, Y.-B., Sachs, L.M., 2013. Mechanisms of thyroid

hormone receptor action during development: lessons from amphibian studies. Biochim. Biophys. Acta 1830 (7), 3882–3892. https://doi.org/10.1016/j.bbagen.2012.04.020.
Hamlet, M.R., Yergeau, D.A., Kuliyev, E., Takeda, M., Taira, M., Kawakami, K., Mead, P.E., 2006. Tol2 transposon-mediated transgenesis in *Xenopus tropicalis*. Genesis 44 (9), 438–445. https://doi.org/10.1002/dvg.20234.
Hasebe, T., Buchholz, D.R., Shi, Y.-B., Ishizuya-Oka, A., 2011. Epithelial-connective tissue interactions induced by thyroid hormone receptor are essential for adult stem cell development in the *Xenopus laevis* intestine. Stem Cells 29 (1), 154–161. https://doi.org/10.1002/stem.560.
Hasebe, T., Fujimoto, K., Kajita, M., Fu, L., Shi, Y.-B., Ishizuya-Oka, A., 2017a. Thyroid hormone-induced activation of Notch signaling is required for adult intestinal stem cell development during *Xenopus laevis* metamorphosis. Stem Cells 35 (4), 1028–1039. https://doi.org/10.1002/stem.2544.
Hasebe, T., Fujimoto, K., Kajita, M., Ishizuya-Oka, A., 2017b. Essential roles of thyroid hormone-regulated hyaluronan/CD44 signaling in adult stem cell development during *Xenopus laevis* intestinal remodeling. Stem Cells 35 (10), 2175–2183. https://doi.org/10.1002/stem.2671.
Hasebe, T., Hartman, R., Fu, L., Amano, T., Shi, Y.-B., 2007. Evidence for a cooperative role of gelatinase A and membrane type-1 matrix metalloproteinase during *Xenopus laevis* development. Mech. Dev. 124 (1), 11–22. https://doi.org/10.1016/j.mod.2006.09.001.
Hasebe, T., Kajita, M., Shi, Y.-B., Ishizuya-Oka, A., 2008. Thyroid hormone-up-regulated hedgehog interacting protein is involved in larval-to-adult intestinal remodeling by regulating sonic hedgehog signaling pathway in *Xenopus laevis*. Dev. Dyn. 237 (10), 3006–3015. https://doi.org/10.1002/dvdy.21698.
Hirsch, C.L., Wrana, J.L., Dent, S.Y.R., 2017. KATapulting toward pluripotency and cancer. J. Mol. Biol. 429 (13), 1958–1977. https://doi.org/10.1016/j.jmb.2016.09.023.
Hourdry, J., Dauca, M., 1977. Cytological and cytochemical changes in the intestinal epithelium during anuran metamorphosis. Int. Rev. Cytol. (Supple.) 5, 337–385.
Ikuzawa, M., Shimizu, K., Yasumasu, S., Iuchi, I., Shi, Y.-B., Ishizuya-Oka, A., 2006. Thyroid hormone-induced expression of a bZip-containing transcription factor activates epithelial cell proliferation during *Xenopus* larval-to-adult intestinal remodeling. Dev. Genes Evol. 216 (3), 109–118. https://doi.org/10.1007/s00427-005-0037-4.
Ishizuya-Oka, A., Hasebe, T., 2013. Establishment of intestinal stem cell niche during amphibian metamorphosis. Curr. Top. Dev. Biol. 103, 305–327. https://doi.org/10.1016/B978-0-12-385979-2.00011-3.
Ishizuya-Oka, A., Hasebe, T., Buchholz, D.R., Kajita, M., Fu, L., Shi, Y.-B., 2009. Origin of the adult intestinal stem cells induced by thyroid hormone in *Xenopus laevis*. FASEB J. 23 (8), 2568–2575. https://doi.org/10.1096/fj.08-128124.
Ishizuya-Oka, A., Hasebe, T., Shi, Y.-B., 2010. Apoptosis in amphibian organs during metamorphosis. Apoptosis 15 (3), 350–364. https://doi.org/10.1007/s10495-009-0422-y.
Ishizuya-Oka, A., Kajita, M., Hasebe, T., 2014. Thyroid hormone-regulated Wnt5a/Ror2 signaling is essential for dedifferentiation of larval epithelial cells into adult stem cells in the *Xenopus laevis* intestine. PLoS One 9 (9), e107611. https://doi.org/10.1371/journal.pone.0107611.
Ishizuya-Oka, A., Li, Q., Amano, T., Damjanovski, S., Ueda, S., Shi, Y.-B., 2000. Requirement for matrix metalloproteinase stromelysin-3 in cell migration and apoptosis during tissue remodeling in *Xenopus laevis*. J. Cell Biol. 150 (5), 1177–1188. https://doi.org/10.1083/jcb.150.5.1177.
Ishizuya-Oka, A., Shimizu, K., Sakakibara, S., Okano, H., Ueda, S., 2003. Thyroid hormone-upregulated expression of Musashi-1 is specific for progenitor cells of the adult epithelium during amphibian gastrointestinal remodeling. J. Cell Sci. 116 (Pt 15), 3157–3164. https://doi.org/10.1242/jcs.00616.
Ishizuya-Oka, A., Shimozawa, A., 1991. Induction of metamorphosis by thyroid hormone in anuran small intestine cultured organotypically *in vitro*. Vitro Cell Dev. Biol. 27A (11), 853–857.
Ishizuya-Oka, A., Ueda, S., 1996. Apoptosis and cell proliferation in the *Xenopus* small intestine during metamorphosis. Cell Tissue Res. 286 (3), 467–476. https://doi.org/10.1007/s004410050716.
Kasai, K., Nishiyama, N., Izumi, Y., Otsuka, S., Ishihara, A., Yamauchi, K., 2015. Exposure to 3,3',5-triiodothyronine affects histone and RNA polymerase II modifications, but not DNA methylation status, in the regulatory region of the *Xenopus laevis* thyroid hormone receptor βA gene. Biochem. Biophys. Res. Commun. 467 (1), 33–38. https://doi.org/10.1016/j.bbrc.2015.09.132.
Kazakevych, J., Sayols, S., Messner, B., Krienke, C., Soshnikova, N., 2017. Dynamic changes in chromatin states during specification and differentiation of adult intestinal stem cells. Nucl. Acids Res. 45 (10), 5770–5784. https://doi.org/10.1093/nar/gkx167.
Koo, B.K., Clevers, H., 2014. Stem cells marked by the R-spondin receptor LGR5. Gastroenterology 147 (2), 289–302. https://doi.org/10.1053/j.gastro.2014.05.007.
Leloup, J., Buscaglia, M., 1977. La triiodothyronine: hormone de la metamorphose des amphibians. C R Acad. Sci. 284, 2261–2263.
Li, B., Carey, M., Workman, J.L., 2007. The role of chromatin during transcription. Cell 128 (4), 707–719. https://doi.org/10.1016/j.cell.2007.01.015.
Madara, J.L., Trier, J.S., 1994. Functional morphology of the mucosa of the small intestine, in: L.R., J. (Ed.) Physiology of the Gastrointestinal Tract. Raven Press Ltd., New York, pp. 1577-1622.
Matsuura, K., Fujimoto, K., Fu, L., Shi, Y.-B., 2012. Liganded thyroid hormone receptor induces nucleosome removal and histone modifications to activate transcription during larval intestinal cell death and adult stem cell development. Endocrinology 153 (2), 961–972. https://doi.org/10.1210/en.2011-1736.
Nakajima, K., Tazawa, I., Yaoita, Y., 2018. Thyroid hormone receptor α- and β-knockout *Xenopus tropicalis* tadpoles reveal subtype-specific roles during development. Endocrinology 159 (2), 733–743. https://doi.org/10.1210/en.2017-00601.
Ni, J., Wangensteen, K.J., Nelsen, D., Balciunas, D., Skuster, K.J., Urban, M.D., Ekker, S.C., 2016. Active recombinant Tol2 transposase for gene transfer and gene discovery applications. Mob. DNA 7, 6. https://doi.org/10.1186/s13100-016-0062-z.
Nieuwkoop, P.D., Faber, J., 1967. Normal table of *Xenopus laevis* (Daudin). North-Holland Pub, Amsterdam.
Okada, M., Miller, T.C., Wen, L., Shi, Y.B., 2017. A balance of Mad and Myc expression dictates larval cell apoptosis and adult stem cell development during *Xenopus* intestinal metamorphosis. Cell Death Dis. 8 (5), e2787. https://doi.org/10.1038/cddis.2017.198.
Patterton, D., Hayes, W.P., Shi, Y.-B., 1995. Transcriptional activation of the matrix metalloproteinase gene stromelysin-3 coincides with thyroid hormone-induced cell death during frog metamorphosis. Dev. Biol. 167 (1), 252–262. https://doi.org/10.1006/dbio.1995.1021.
Paul, B.D., Buchholz, D.R., Fu, L., Shi, Y.-B., 2007. SRC-p300 coactivator complex is required for thyroid hormone-induced amphibian metamorphosis. J. Biol. Chem. 282 (10), 7472–7481. https://doi.org/10.1074/jbc.M607589200.
Ranjan, M., Wong, J., Shi, Y.-B., 1994. Transcriptional repression of *Xenopus* TR beta gene is mediated by a thyroid hormone response element located near the start site. J. Biol. Chem. 269 (40), 24699–24705.
Rebel, V.I., Kung, A.L., Tanner, E.A., Yang, H., Bronson, R.T., Livingston, D.M., 2002. Distinct roles for CREB-binding protein and p300 in hematopoietic stem cell self-renewal. Proc. Natl. Acad. Sci. U.S.A. 99 (23), 14789–14794. https://doi.org/10.1073/pnas.232568499.
Sachs, L.M., Buchholz, D.R., 2017. Frogs model man: In vivo thyroid hormone signaling during development. Genesis 55 (1–2). https://doi.org/10.1002/dvg.23000.
Sachs, L.M., Buchholz, D.R., 2019. Insufficiency of thyroid hormone in frog metamorphosis and the role of glucocorticoids. Front. Endocrinol. (Lausanne) 10, 287. https://doi.org/10.3389/fendo.2019.00287.
Sakane, Y., Iida, M., Hasebe, T., Fujii, S., Buchholz, D.R., Ishizuya-Oka, A., Yamamoto, T., Suzuki, K.T., 2018. Functional analysis of thyroid hormone receptor beta in *Xenopus tropicalis* founders using CRISPR-Cas. Biol. Open 7 (1). https://doi.org/10.1242/bio.030338.
Shi, Y.-B., 1999. Amphibian Metamorphosis: From Morphology to Molecular Biology. John Wiley & Sons Inc, New York.
Shi, Y.-B., 2013. Unliganded thyroid hormone receptor regulates metamorphic timing via the recruitment of histone deacetylase complexes. Curr. Top. Dev. Biol. 105, 275–297. https://doi.org/10.1016/B978-0-12-396968-2.00010-5.
Shi, Y.-B., Ishizuya-Oka, A., 1996. Biphasic intestinal development in amphibians: embryogenesis and remodeling during metamorphosis. Curr. Top. Dev. Biol. 32, 205–235.
Shi, Y.-B., Ishizuya-Oka, A., 1997. Autoactivation of *Xenopus* thyroid hormone receptor β genes correlates with larval epithelial apoptosis and adult cell proliferation. J. Biomed. Sci. 4 (1), 9–18. https://doi.org/10.1007/bf02255588.
Shi, Y.-B., Liang, V.C., 1994. Cloning and characterization of the ribosomal protein L8 gene from *Xenopus laevis*. Biochim. Biophys. Acta 1217 (2), 227–228. https://doi.org/10.1016/0167-4781(94)90042-6.
Shibano, T., Takeda, M., Suetake, I., Kawakami, K., Asashima, M., Tajima, S., Taira, M., 2007. Recombinant Tol2 transposase with activity in *Xenopus* embryos. FEBS Lett. 581 (22), 4333–4336. https://doi.org/10.1016/j.febslet.2007.08.004.
Sirakov, M., Boussouar, A., Kress, E., Frau, C., Lone, I.N., Nadjar, J., Angelov, D., Plateroti, M., 2015. The thyroid hormone nuclear receptor TRα1 controls the Notch signaling pathway and cell fate in murine intestine. Development 142 (16), 2764–2774. https://doi.org/10.1242/dev.121962.
Sirakov, M., Plateroti, M., 2011. The thyroid hormones and their nuclear receptors in the gut: from developmental biology to cancer. Biochim. Biophys. Acta 1812 (8), 938–946. https://doi.org/10.1016/j.bbadis.2010.12.020.
Sirakov, M., Skah, S., Nadjar, J., Plateroti, M., 2013. Thyroid hormone's action on progenitor/stem cell biology: new challenge for a classic hormone? Biochim. Biophys. Acta 1830 (7), 3917–3927. https://doi.org/10.1016/j.bbagen.2012.07.014.
Suh, J.H., Sieglaff, D.H., Zhang, A., Xia, X., Cvoro, A., Winnier, G.E., Webb, P., 2013. SIRT1 is a direct coactivator of thyroid hormone receptor beta1 with gene-specific actions. PLoS One 8 (7), e70097. https://doi.org/10.1371/journal.pone.0070097.
Sun, G., Hasebe, T., Fujimoto, K., Lu, R., Fu, L., Matsuda, H., Kajita, M., Ishizuya-Oka, A., Shi, Y.-B., 2010. Spatio-temporal expression profile of stem cell-associated gene LGR5 in the intestine during thyroid hormone-dependent metamorphosis in *Xenopus laevis*. PLoS One 5 (10), e13605. https://doi.org/10.1371/journal.pone.0013605.
Swigut, T., Wysocka, J., 2007. H3K27 demethylases, at long last. Cell 131 (1), 29–32. https://doi.org/10.1016/j.cell.2007.09.026.
Wang, T., Liu, H., Ning, Y., Xu, Q., 2014. The histone acetyltransferase p300 regulates the expression of pluripotency factors and odontogenic differentiation of human dental pulp cells. PLoS One 9 (7), e102117. https://doi.org/10.1371/journal.pone.0102117.
Wang, X., Matsuda, H., Shi, Y.-B., 2008. Developmental regulation and function of thyroid hormone receptors and 9-cis retinoic acid receptors during *Xenopus tropicalis* metamorphosis. Endocrinology 149 (11), 5610–5618. https://doi.org/10.1210/en.2008-0751.
Wen, L., Fu, L., Shi, Y.-B., 2017. Histone methyltransferase Dot1L is a coactivator for thyroid hormone receptor during *Xenopus* development. FASEB J. 31 (11), 4821–4831. https://doi.org/10.1096/fj.201700131R.
Wen, L., Shi, Y.-B., 2016. Regulation of growth rate and developmental timing by *Xenopus* thyroid hormone receptor alpha. Dev. Growth Differ. 58 (1), 106–115. https://doi.org/10.1111/dgd.12231.
Wong, J., Shi, Y.-B., 1995. Coordinated regulation of and transcriptional activation by *Xenopus* thyroid hormone and retinoid X receptors. J. Biol. Chem. 270 (31), 18479–18483. https://doi.org/10.1074/jbc.270.31.18479.